AD-A170 906 PREDICTED EFFECT OF DYNAMIC LOAD ON PITTING FATIGUE LIFE FOR LOW-CONTACT-...(U) NATIONAL AERONAUTICS AND SPACE ADMINISTRATION CLEVELAND OH LE.. D G LEWICKI 1/1

UNCLASSIFIED JUN 86 NASA-E-2989 NASA-TP-2610 F/G 13/9 NL

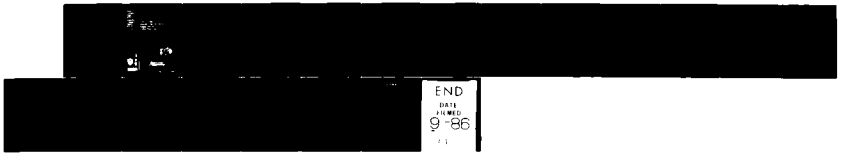

END

DATE FILMED

9-86

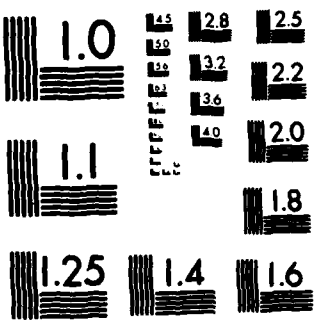

NASA
Technical
Paper
2610

AVSCOM
Technical
Report
86-C-21

June 1986

Predicted Effect of Dynamic Load on Pitting Fatigue Life for Low-Contact-Ratio Spur Gears

David G. Lewicki

NASA

Summary

How dynamic load affects the pitting fatigue life of external spur gears was predicted by using NASA computer program TELSGE. TELSGE was modified to include an improved gear tooth stiffness model, a stiffness–dynamic load iteration scheme, and a pitting-fatigue-life prediction analysis for a gear mesh. The analysis used the NASA gear life model developed by Coy, methods of probability and statistics, and gear tooth dynamic loads to predict life. In general, gear life predictions based on dynamic loads differed significantly from those based on static loads, with the predictions being strongly influenced by the maximum dynamic load during contact.

With the modified TELSGE, parametric studies were performed that modeled low-contact-ratio involute spur gears over a range of gear speeds, numbers of teeth, gear sizes, diametral pitches, pressure angles, and gear ratios. Dynamic loads and pitting fatigue lives were calculated. Gear mesh operating speed strongly affected predicted dynamic load and life. Meshes operating at a resonant speed or at one-half the resonant speed had significantly shorter lives. Dynamic life factors for gear surface pitting fatigue were developed on the basis of the parametric studies. The effects of number of teeth, gear size, diametral pitch, pressure angle, and gear ratio on predicted life were related to the contact ratio. In general, meshes with higher contact ratios had higher dynamic life factors than meshes with lower contact ratios. A design chart was developed for use in the absence of a computer and program TELSGE. An example illustrates the use of the design chart.

Introduction

Gears may fail from scoring, tooth fracture due to bending fatigue, or surface pitting fatigue. Scoring failure is usually lubrication related and can be prevented by proper lubrication and proper operating temperatures. Tooth fractures are usually caused by poor materials, improper design, or overloading and can be prevented by designing for bending stresses below the material's maximum allowable stress. The American Gear Manufacturers Association (AGMA) has a standard practice for predicting gear surface pitting fatigue (ref. 1). The method assumes that infinite life results when the maximum surface contact stresses are less than the material's endurance limit. Surface contact stress calculations may include a dynamic factor to account for gear dynamic loading. The AGMA recommends a dynamic factor of 1 for gear teeth of high accuracy but states that actual dynamic loads, computed or measured, can be used (ref. 1).

Gear research authorities do not completely agree on surface pitting fatigue. Some state that gear materials do not have surface endurance limits (refs. 2 and 3), as is true for rolling-element bearings. In 1975, Coy developed an improved model for the surface fatigue life of spur and helical gears, using an approach similar to that for rolling-element bearings (refs. 2 to 6). This work did not, however, include the effect of dynamic load.

Early contributions to gear dynamic loading were made by Buckingham, Tuplin, Richardson, and Attia (refs. 7 to 10). More recently computer-based analytical programs have been developed to determine gear tooth dynamic loads (refs. 11 to 16). The dynamic loads of these programs depend on such factors as inertia and stiffness of rotating members, tooth spacing and profile errors, size, and speed. The loads are determined by solving the equations of motion of a given gear mesh system.

The objective of the present study was to combine the dynamic load calculation procedure of Wang and Cheng (ref. 14) with the NASA gear life model of Coy (refs. 2 to 6) to determine how dynamic load affects the pitting fatigue life of external spur gears. NASA computer program TELSGE, modified to include Cornell's gear tooth stiffness model (ref. 17), a stiffness–dynamic load iteration scheme, and a pitting fatigue life analysis, was used to predict gear dynamic loads and life. Parametric studies using modified TELSGE were performed for low-contact-ratio involute gears with no tooth spacing or profile errors. Gear dynamic loads and tooth stiffnesses were calculated as a function of contact position and speed. On the basis of the parametric studies dynamic life factors for gear surface pitting fatigue were developed as a function of speed and contact ratio.

Analysis

Gear Life Model

Current theory.—The life model proposed by Lundberg and Palmgren (refs. 18 to 20) is the commonly accepted theory for predicting the pitting fatigue life of rolling-element bearings. Because the fatigue failure mechanism is similar for both gears and rolling-element bearings made from high-

strength steel, the Lundberg-Palmgren model for bearings has been adapted to predict gear life (refs. 2 to 6). Reference 6 gives the life for a 90-percent probability of survival η of a single tooth on a driver or driven gear of a mesh as

$$\eta = B^{4.3} f^{3.9} \Sigma\rho^{-5} \ell^{-0.4} Q^{-4.3} \tag{1}$$

where B is a material constant based on experimental data; f is the tooth face width; $\Sigma\rho$ is the curvature sum at the start of single-tooth contact; ℓ is the involute surface length during single-tooth contact; and Q is the static tooth load, normal to the contact. A complete list of symbols is given in appendix A.

The life of the complete driver gear (all teeth) L_1 in terms of driver gear rotations is

$$L_1 = N_1^{-1/e} \eta \tag{2}$$

where N_1 is the number of teeth on the driver gear and e, the Weibull exponent, is a measure of scatter in fatigue life. Experimental research on AISI 9310 steel spur gears has shown gear fatigue to follow the Weibull failure distribution with $e \approx 2.5$ (ref. 3).

The life of the complete driven gear L_2 in terms of driver gear rotations is

$$L_2 = \left(\frac{N_2}{N_1}\right) N_2^{-1/e} \eta \tag{3}$$

where N_2 is the number of teeth on the driven gear. The mesh life (both driver and driven gears) L_m in terms of driver gear rotations is given by

$$L_m = \left(L_1^{-e} + L_2^{-e}\right)^{-1/e} \tag{4}$$

Expanded theory.—To adapt the current gear life model for predictions based on gear tooth dynamic loads, the tooth was divided into intervals (fig. 1). The use of intervals allowed the current gear life model to account for load and curvature sums varying with contact position. The complete gear tooth life was determined from the interval lives and methods of probability and statistics. The details are as follows.

When a pair of external spur gears is in mesh (fig. 2), the line tangent to the base circles of both the driver and driven gears is called the line of action. The gears begin contact when the outside radius of the driven gear intersects the line of action. As the gears rotate, the contact point occurs on the line of action. The contact ends when the outside radius of the driver gear intersects the line of action. The point at which the pitch circles of the driver and driven gears intersect is called the pitch point. The distance along the line of action from the pitch point to the start of contact is

$$z_1 = \sqrt{r_{o,2}^2 - r_{b,2}^2} - r_{p,2} \sin\varphi \tag{5}$$

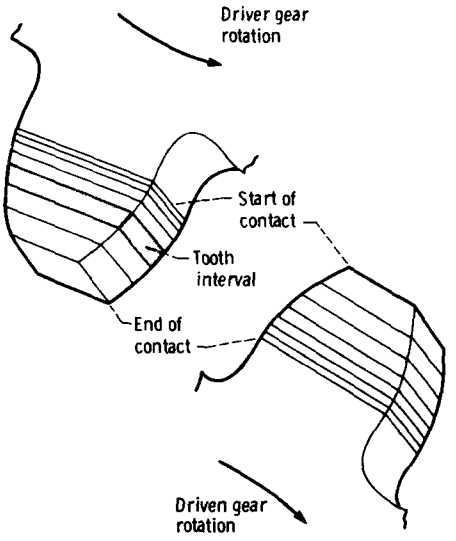

Figure 1.—Tooth intervals of a meshing gear pair.

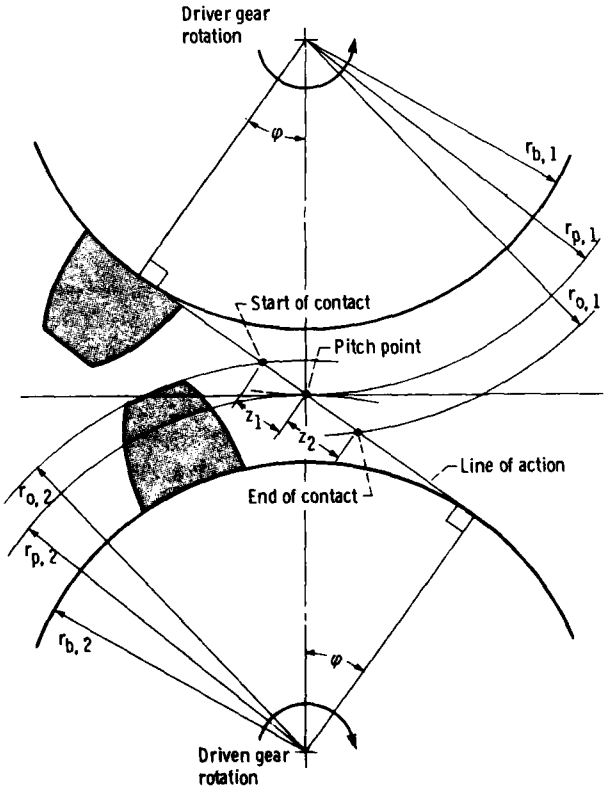

Figure 2.—Basic geometry of a pair of external spur gears in mesh.

The distance along the line of action from the pitch point to the end of contact is

$$z_2 = \sqrt{r_{o,1}^2 - r_{b,1}^2} - r_{p,1} \sin\varphi \tag{6}$$

The contact length Z is defined as

$$Z = z_1 + z_2 \tag{7}$$

Dividing the contact length into equal-size intervals of length Δx gives

$$\Delta x = \frac{Z}{J} \tag{8}$$

where J is the total number of intervals on a tooth, and

$$x_i = -z_1 + (i-1)\Delta x \qquad \text{for } i = 1 \text{ to } J+1 \tag{9}$$

where x is the contact position along the line of action. The value of x is negative when contact is before the pitch point, zero when at the pitch point, and positive when after the pitch point.

The life of each interval for a 90-percent probability of survival is given from equation (1) by

$$\eta_j = B^{4.3} f^{3.9} \overline{\Sigma\rho_j}^{-5} \ell_j^{-0.4} \overline{Q}_j^{-4.3} \qquad \text{for } j = 1 \text{ to } J \tag{10}$$

where B and f do not change from interval to interval. Both curvature sum and involute length, however, change with contact position.

At the i^{th} contact position the radii of curvature of the driver and driven gears (fig. 3) are

$$R_{1,i} = r_{p,1} \sin\varphi + x_i \tag{11}$$

$$R_{2,i} = r_{p,2} \sin\varphi - x_i \tag{12}$$

The curvature sum at the i^{th} contact position is

$$\Sigma\rho_i = \frac{1}{R_{1,i}} + \frac{1}{R_{2,i}} \tag{13}$$

For the j^{th} interval the average curvature sum used in the life model is

$$\overline{\Sigma\rho_j} = \frac{\Sigma\rho_i + \Sigma\rho_{i+1}}{2} \qquad \text{for } i = j \tag{14}$$

The curvature sum varied slightly with contact position for the example gear mesh data from table I for 100 intervals on each tooth (fig. 4(a)). (The contact position was made dimensionless by dividing by the base pitch p_b.) The plot shows the curvature sum to be symmetric about the pitch point ($x = 0$). This was true only because the driver and driven gears of the example were the same size.

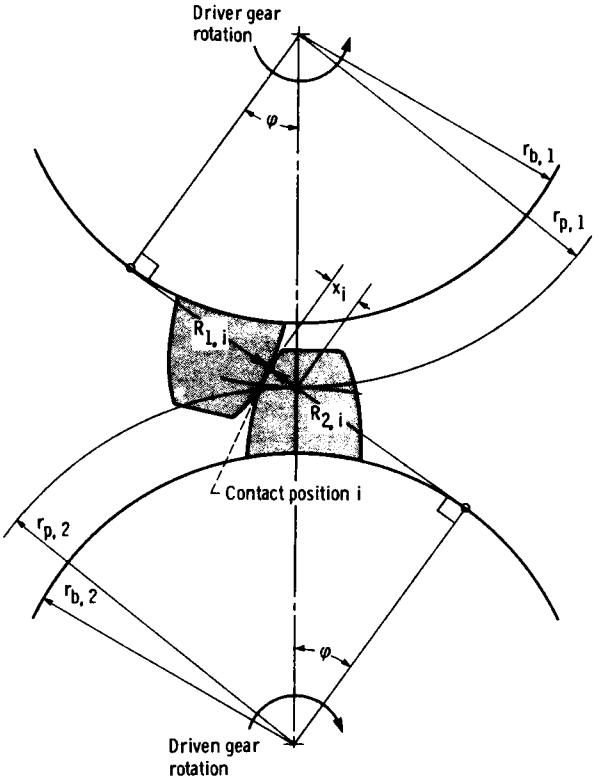

Figure 3.—Curvatures of involute teeth in contact.

TABLE I.—BASELINE DATA FOR BOTH DRIVER AND DRIVEN GEAR

Number of teeth	36
Diametral pitch	8
Outside radius, cm (in.)	6.033 (2.375)
Base pitch, cm (in.)	0.937 (0.369)
Face width, cm (in.)	0.635 (0.250)
Pressure angle, deg	20
Root radius, cm (in.)	5.318 (2.094)
Fillet radius, cm (in.)	0.102 (0.040)
Chordal tooth thickness, cm (in.)	0.485 (0.191)
Normal load, N (lb)	1718 (386)
Speed, rpm	4000
Material	Steel

The involute surface lengths of the driver and driven gears for the j^{th} interval (for small Δx) are

$$\ell_{1,j} = \left(\frac{\Delta x}{r_{b,1}}\right) x_i + \Delta x \tan\varphi \qquad \text{for } i = j \tag{15}$$

$$\ell_{2,j} = -\left(\frac{\Delta x}{r_{b,2}}\right) x_i + \Delta x \tan\varphi \qquad \text{for } i = j \tag{16}$$

The involute length is a linear function of contact position (fig. 4(b)). Equations (15) and (16) imply that rotating a gear mesh

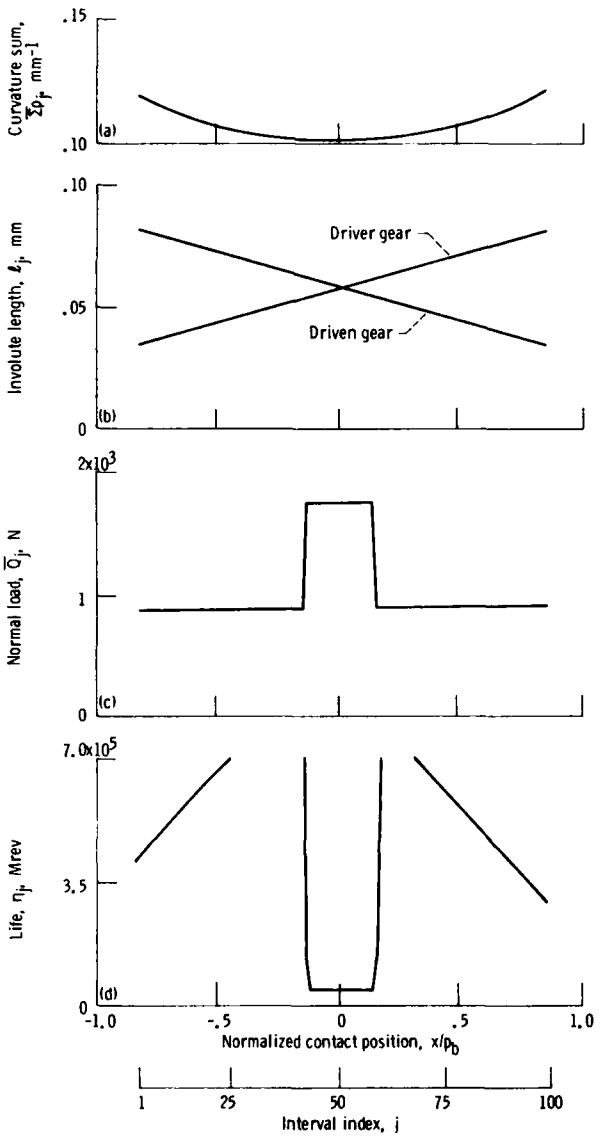

(a) Average curvature sum of interval.
(b) Length of involute surface of interval.
(c) Average normal load on interval.
(d) Life of interval for driver gear. Tooth life, 13 200 Mrev; gear life, 3100 Mrev; mesh life, 2400 Mrev.

Figure 4.—Effect of contact position on gear life parameters for gear data from table I.

through equal angles produces unequal involute lengths and thus different-size tooth intervals (as shown in fig. 1).

By using intervals the life model considers load that can vary with contact position. For the j^{th} interval the average load used in the life model is

$$\bar{Q}_j = \frac{Q_i + Q_{i+1}}{2} \qquad \text{for } i = j \tag{17}$$

The static load variation with contact position depends on the number of teeth in contact (fig. 4(c)). As a pair of teeth begin contact, the preceding pair of mating teeth are also in contact. This double-tooth-pair contact occurs for intervals 1 to 41, and it is assumed that half the applied load is transferred per contact. Near the pitch point single-tooth-pair contact occurs (intervals 42 to 59), and all the load is transferred by it. Toward the end of contact, double-tooth-pair contact again occurs (intervals 60 to 100) as the following pair of mating teeth begin contact. As before, it is assumed that half the load is transferred per contact.

The life of a complete gear tooth η_t is determined from the interval lives and methods of probability and statistics where

$$\eta_t = \left(\sum_{j=1}^{J} \eta_j^{-e} \right)^{-1/e} \tag{18}$$

The complete tooth life was always shorter than the lives of the shortest-lived intervals (fig. 4(d)). Also, intervals with larger applied loads had much more influence on gear tooth life than intervals with smaller loads.

The tooth lives for a driver and driven gear in mesh are determined by the expanded life theory and equation (18). They are equal if the driver and driven gears are the same size. They are slightly different if the driver and driven gears are different sizes because of curvature sums and involute lengths. The complete gear lives and mesh life are determined, as before, by using equations (2) to (4) and substituting η_t for η.

The total number of tooth intervals was varied from 30 to over 400 to check convergence on life. Static loads were used. All cases predicted the same tooth life. Gear size, diametral pitch, pressure angle, and gear ratio were also varied to compare mesh lives predicted by the current and expanded theories. Static loads were used. The expanded theory predicted mesh lives a little longer than, but within 10 percent of, those predicted by the current theory for meshes with equal-size gears. This difference was caused by the expanded theory's curvature sum variation with contact position. Thus for meshes with equal-size gears the curvature sum variation had a small effect on life. For meshes with unequal-size gears, however, there were greater differences in the mesh lives predicted by the two theories.

Gear Tooth Dynamic Loads

Gear tooth dynamic load model.—The contact load of meshing gear teeth varies as the contact point moves along the line of action. This is known as dynamic load. It is mainly caused by single- and double-tooth-pair contact transitions, tooth stiffness variation along the contact, and tooth profile deviations from true involutes (tooth profile errors). NASA computer program TELSGE (refs. 14 to 16) was used to determine gear tooth dynamic loads. The program models meshing gears as a pair of rigid disks connected by a spring

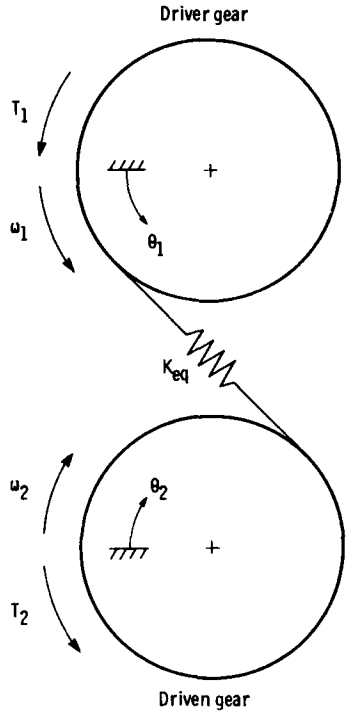

Figure 5.—Dynamic model of meshing gears.

(fig. 5). The spring stiffness corresponds to gear teeth stiffnesses.

The dynamic load model uses the equations of motion governing the angular displacements of the driver and driven gears. By converting the angular movements of the disks to linear displacements along the line of action, and by algebraic manipulation, the equations of motion are represented by a single differential equation, where

$$M_{eq}\ddot{X} + C_{eq}\dot{X} + K_{eq}X = P_s \tag{19}$$

The dependent variable X, called the relative displacement, is the compression of the spring along the line of action,

$$X = s_1 - s_2 \tag{20}$$

where

$$s_1 = r_{b,1}\theta_1 \quad \text{and} \quad s_2 = r_{b,2}\theta_2 \tag{21}$$

The equivalent mass per unit face width is

$$M_{eq} = \frac{M_1 M_2}{M_1 + M_2} \tag{22}$$

The equivalent damping coefficient per unit face width C_{eq} includes the effect of viscous damping,

$$C_{eq} = 2\zeta\sqrt{K_{eq}M_{eq}} \tag{23}$$

where ζ is the damping ratio, K_{eq} is the equivalent stiffness per unit face width (discussed in the section ***Equivalent gear tooth stiffness***), and P_s is the static load per unit face width.

The relative displacement is determined as a function of contact position by using a Runge-Kutta numerical method and solving equation (19). The dynamic load on a gear tooth is determined as a function of contact position by

$$P_d = KX \tag{24}$$

where P_d is the dynamic load per unit face width and K is the combined stiffness per unit face width (discussed in the section ***Equivalent gear tooth stiffness***). Note that when X is negative, the teeth separate and the dynamic load is zero. Although tooth profile errors can be accounted for in equations (19) and (24), they were beyond the scope of this study.

Gear tooth stiffness.—Computer program TELSGE was modified to incorporate the gear tooth stiffness model of Cornell (ref. 17), regarded as the present state of the art. The stiffness model consists of tooth bending as a cantilever beam, fillet and foundation flexibilities, and local Hertzian compression, all as functions of contact position. In Cornell's model the deflections due to bending and fillet and foundation flexibilities are expressed as linear functions of load, but the deflections due to Hertzian effects are not linear with load. This makes the stiffness of a gear tooth dependent on dynamic load, and equation (19) nonlinear.

Equivalent gear tooth stiffness.—The stiffnesses of the driver and driven teeth of a mesh, k_1 and k_2 respectively, are found by the methods of Cornell (ref. 17). The combined stiffness K for a pair of teeth in contact is

$$K = \frac{k_1 k_2}{k_1 + k_2} \tag{25}$$

For a single pair of teeth in contact (fig. 6(a)) the equivalent stiffness is

$$K_{eq} = \mathrm{K} \tag{26}$$

For two pairs of teeth in contact (fig. 6(b)) the equivalent stiffness is

$$K_{eq} = K^{(\mathrm{I})} + K^{(\mathrm{II})} \tag{27}$$

where

$$K^{(\mathrm{I})} = \frac{k_1^{(\mathrm{I})} k_2^{(\mathrm{I})}}{k_1^{(\mathrm{I})} + k_2^{(\mathrm{I})}} \tag{28}$$

$$K^{(\mathrm{II})} = \frac{k_1^{(\mathrm{II})} k_2^{(\mathrm{II})}}{k_1^{(\mathrm{II})} + k_2^{(\mathrm{II})}} \tag{29}$$

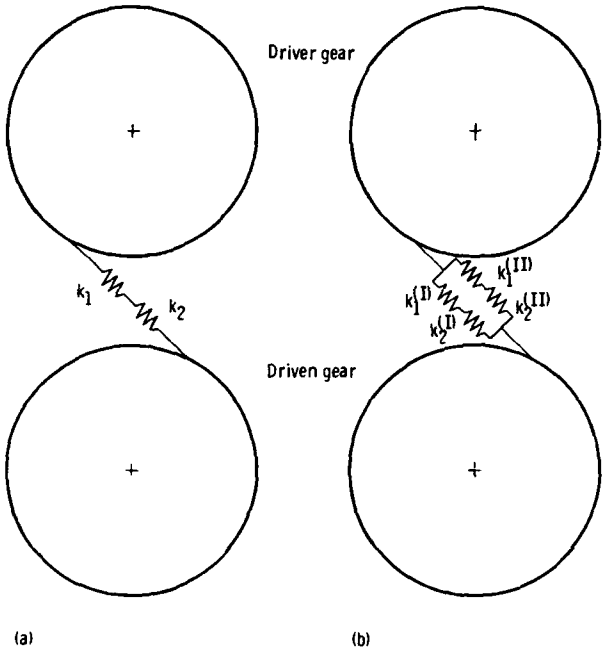

(a) Single-tooth-pair contact.
(b) Double-tooth-pair contact.

Figure 6.—Gear tooth stiffness models.

The superscript (I) refers to the first pair of teeth in contact and (II) refers to the second pair of teeth in contact. The equivalent stiffness of equation (19) varies from double-tooth-pair contact at the start of mesh to single-tooth-pair contact and back to double.

Iteration of gear tooth stiffness and dynamic load.— Because of the Hertzian compression, gear tooth stiffness is not independent of dynamic load. TELSGE was therefore modified to iterate for dynamic load (fig. 7). First the static load is defined. As in the example (fig. 4(c)) all the load is transferred per contact during single-tooth-pair contact, and half the load is transferred per contact during double-tooth-pair contact. Next the combined stiffness is determined along the contact position by using the static load in the Hertzian deflection computation. Then the dynamic load is determined along the contact position. Next combined stiffness is recalculated by using the calculated dynamic load in the Hertzian deflection computation. Then dynamic load is recalculated by using the latest stiffness values. The stiffness and load calculations continue until the change in dynamic load with each iteration becomes smaller than a preset amount.

With modified TELSGE and the example data (table I) the dynamic load required only four iterations to converge to within 0.1 percent (fig. 8). So few iterations were required since the Hertzian deflection was usually only 10 to 20 percent of the total gear tooth deflection. The variation in equivalent stiffness due to double- and single-tooth-pair contact transitions is a major excitation in the dynamic load model (fig. 9). The dynamic load varied appreciably from the static when the operating conditions of the example were used (fig. 10). The maximum dynamic load during contact was about 30 percent greater than the static load.

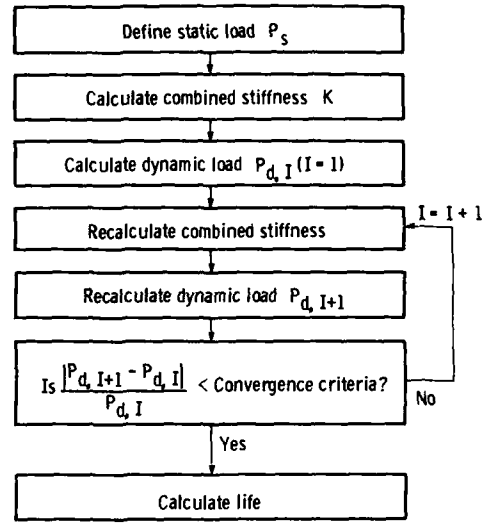

Figure 7.—Flowchart of gear tooth combined stiffness–dynamic load interaction scheme in computer program TELSGE.

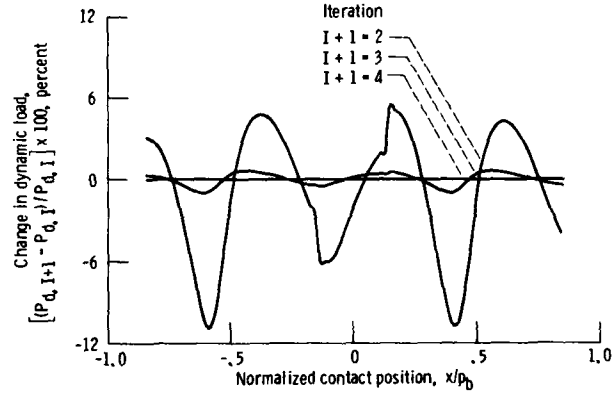

Figure 8.—Effect of gear tooth combined stiffness–dynamic load interation scheme on dynamic load for gear data from table I.

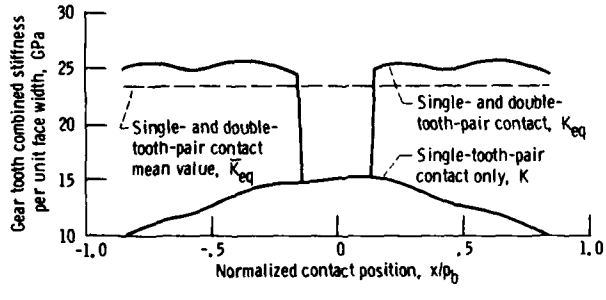

Figure 9.—Effect of contact position on gear tooth combined stiffness for gear data from table I.

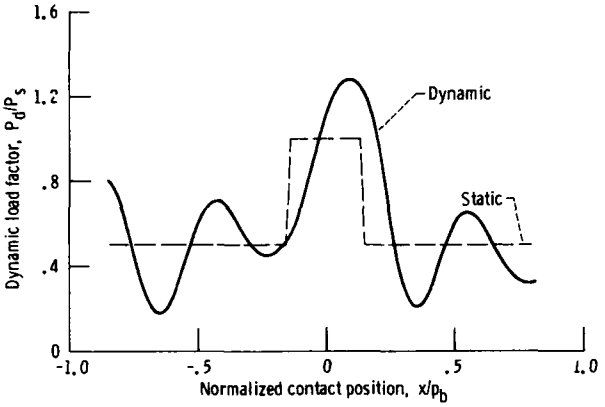

Figure 10.—Effect of contact position on gear tooth dynamic load for gear data from table I.

Gear life using dynamic loads.—The expanded gear life model, which accounts for variations of load and curvature sums with respect to contact position, was incorporated in modified TELSGE. The dynamic loads were used in the life model, where

$$Q_i = P_{d,i} f \qquad \text{for } i = 1 \text{ to } 101 \qquad (30)$$

(TELSGE divides the contact length into 100 intervals.) For the data from table I the mesh life based on dynamic loads was then 50 percent shorter than that based on static loads. The cause was the increase in maximum load during contact when dynamic loads were considered (fig. 10).

Results and Discussion

NASA computer program TELSGE, modified to include an improved gear tooth stiffness model, a tooth stiffness–dynamic load iteration scheme, and a pitting fatigue life prediction method, was used to perform parametric studies. Dynamic loads and gear mesh life predictions were performed over a range of gear speeds, numbers of teeth, gear sizes, diametral pitches, pressure angles, and gear ratios.

Effect of Speed on Dynamic Load and Life

Modified TELSGE was run using the mesh data in table I for speeds ranging from 600 to 12 000 rpm. At very low speeds the dynamic load as a function of contact position (fig. 11) resembled the static load. However, spikes occurred at double- to single-tooth-pair contact transitions, and at single

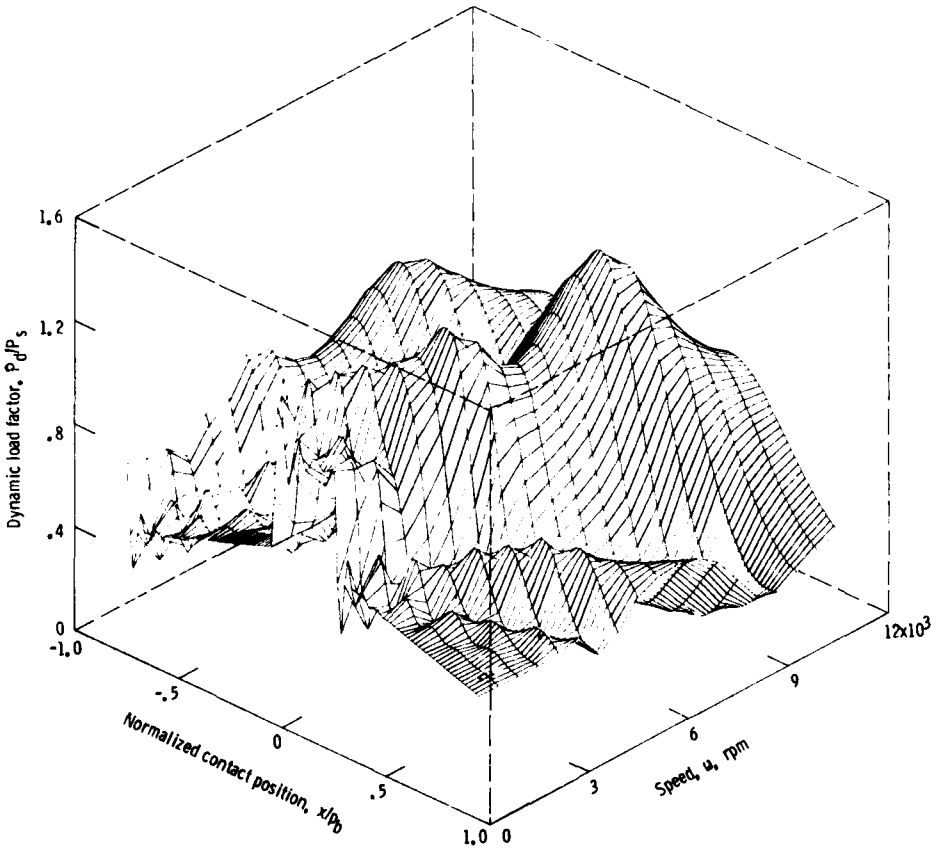

Figure 11.—Effect of contact position and speed on gear tooth dynamic load for gear data from table I.

to double. As the speed increased, the dynamic load as a function of contact position differed appreciably from the static.

The dynamic load reached a maximum at a resonant speed ω_n of about 8500 rpm. At speeds below resonance the excitation frequency from the change in equivalent stiffness was lower than the resonant frequency, and the dynamic load was basically an oscillatory load superimposed on the static load. This produced peak dynamic loads greater than the static load. At speeds above resonance the dynamic load had a smoother response, with peaks lower than the static. This was caused by the greater inertia forces at higher speeds. The resonant speed can be approximated by

$$\omega_n = \frac{\sqrt{\bar{K}_{eq}/M_{eq}}\cos\varphi}{N}\left(\frac{60}{2\pi}\right) \tag{31}$$

Here although the mean equivalent stiffness K_{eq} varies with load and speed due to Hertzian effects, its influence on ω_n is not significant.

For the data in figure 11 the maximum dynamic load during contact was greatest at the resonant speed (fig. 12). It was also greater than the static load at speeds below resonance, with a secondary peak at about $\omega/\omega_n = 0.5$. At speeds above resonance the maximum dynamic load during contact decreased and was less than the static load above $\omega/\omega_n \approx 1.2$.

The gear mesh life as a function of speed for the mesh data in table I is shown in figure 13. The dynamic life factor is defined as

$$C_v = \frac{L_d}{L_s} \tag{32}$$

where L_d is the gear mesh life based on the expanded life theory and dynamic loads and L_s is the gear mesh life based on the expanded life theory and static loads (as illustrated in fig. 4). Comparing figures 12 and 13 shows that the gear mesh life decreased when the maximum dynamic load during contact increased. This was true even though the analysis considered

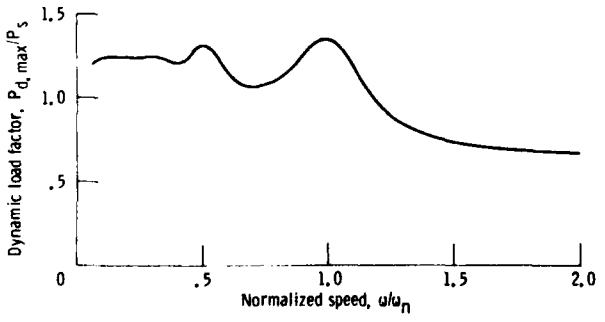

Figure 12.—Effect of speed on maximum gear tooth dynamic load during contact for gear data from table I.

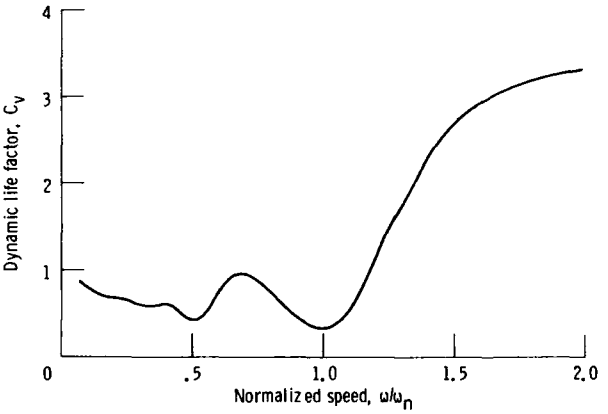

Figure 13.—Effect of speed on gear mesh life for gear data from table I.

the load along the complete contact length. The mesh life as a function of speed was lowest at resonance.

Effect of Mass, Stiffness, and Damping on Gear Life

The mass, stiffness, and damping of a gear mesh system significantly affected dynamic load and life. Modified TELSGE was run using the mesh data in table I while varying the equivalent mass M_{eq} and keeping all other parameters the same. The life-speed results were identical when plotted on dimensionless coordinates (as in fig. 13). Modified TELSGE was also run while varying the equivalent stiffness K_{eq} and keeping all other parameters the same. Again, the life-speed results were identical when plotted on dimensionless coordinates (as in fig. 13). Thus the value of the equivalent mass or the equivalent stiffness had no effect on the life-speed results when plotted on dimensionless coordinates. However, as expected from equation (31), different values of the equivalent mass or the equivalent stiffness produced different values for the resonant speed. The equivalent mass and equivalent stiffness must accurately portray the gear mesh being modeled for the calculated resonant speed to be accurate.

The damping force in the dynamic load model depends on the gear system's viscous friction and is usually an unknown. Damping ratios ζ between 0.1 (in eq. (23)) and 0.2 were used in reference 11 to correlate analytical and experimental dynamic load gear tests. Here damping ratios of 0.10, 0.17, and 0.25 were used (fig. 14). Decreasing the damping ratio increased the dynamic load and thus shortened the mesh life at speeds near the resonant speed and one-half the resonant speed (ω/ω_n = 1.0 and 0.5, respectively). A damping ratio of 0.17 was used in the original version of TELSGE and was used in this study for all other figures.

Effect of Speed and Contact Ratio on Gear Life

Modified TELSGE was used to predict how speed and contact ratio affect dynamic load and gear life. Number of teeth, gear size, diametral pitch, pressure angle, and gear ratio

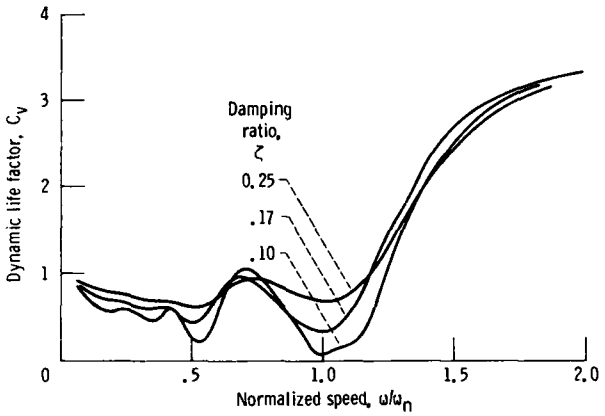

Figure 14.—Effect of damping ratio on gear mesh life for gear data from table I.

were varied. The driver gear data for the different runs are shown in table II. The different sets had basically the same shape while displaced upward or downward when plotted on dimensionless life-speed coordinates (fig. 15). In most sets the mesh life was shortest at the resonant speed or one-half the resonant speed and was significantly shorter than the life based on static loads at those speeds. For all sets meshes operating above resonance had significantly longer life when compared with the static load calculations.

TABLE II.—DRIVER GEAR DATA

[Set 1 used for baseline; shaded area indicates parameter varied from baseline.]

Set	Number of teeth	Pitch radius, cm	Diametral pitch	Pressure angle, deg	Gear ratio	Contact ratio
1	36	5.715	8	20	1	1.69
2	20	3.175				1.56
3	28	4.445				1.64
4	44	6.985				1.73
5	52	8.255				1.76
6	60	9.525				1.78
7	66	6.985	12			1.80
8	99	6.985	18			1.85
9	28	4.445	8	14.5		1.92
10	20	3.175		25		1.41
11	28	4.445		25		1.46
12	36	5.715		25		1.50
13	36	5.715		20	2	1.75
14	36	5.715		20	3	1.78

The contact ratio c, defined as the average number of teeth pairs in contact, is given by

$$c = \frac{Z}{p_b} \tag{33}$$

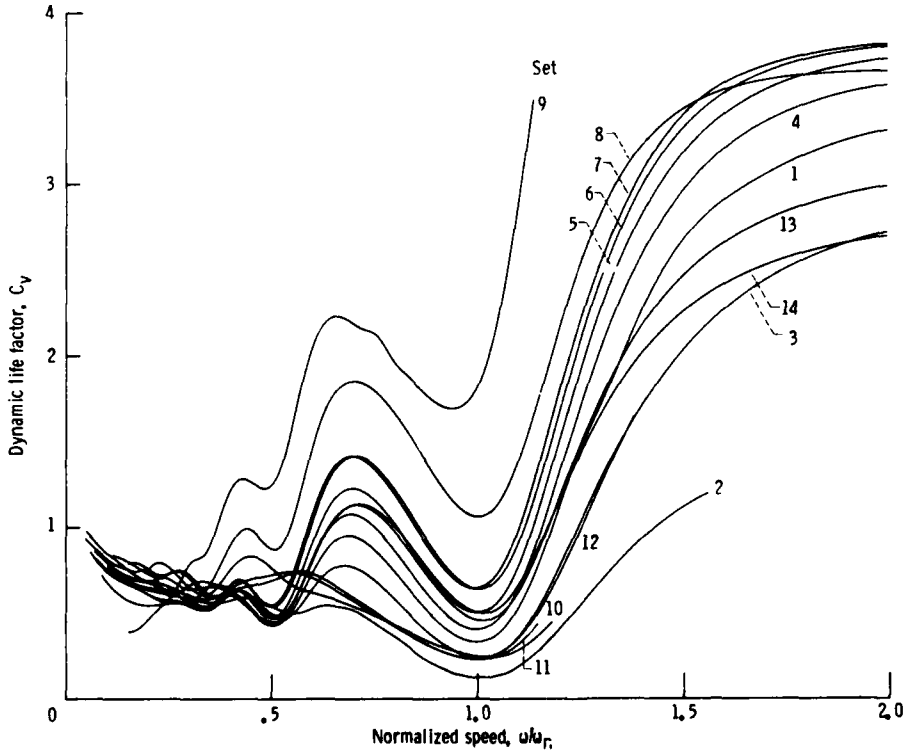

Figure 15.—Effect of speed on gear mesh life for parametric study data from table II.

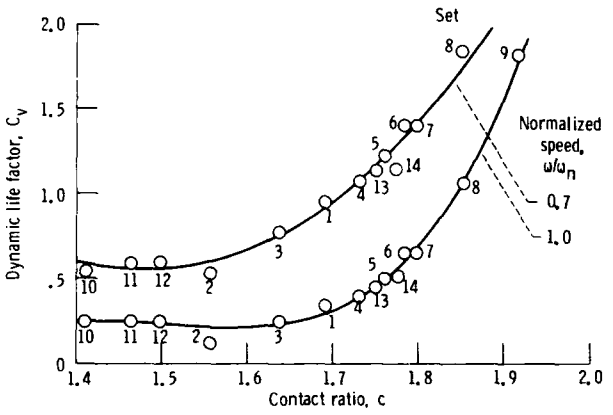

Figure 16.—Effect of contact ratio on gear mesh life for parametric study data from table II.

For a mesh with a contact ratio of 1.6, two pairs of teeth are in contact 60 percent of the time and one pair is in contact 40 percent of the time. Low-contact-ratio gears have contact ratios between 1 and 2. In the parametric studies the contact ratio ranged from 1.41 to 1.92.

For the data in figure 15 the dynamic life factor was plotted as a function of contact ratio in figure 16 for speeds ω/ω_n of 0.7 and 1.0. A sixth-order polynomial curve-fit was used to generate the curves. At a constant normalized speed the dynamic life factors were about the same for meshes with contact ratios between 1.4 and 1.6 but were significantly higher for meshes with higher contact ratios.

With higher contact ratios the equivalent stiffness (fig. 9) had a smaller duration of single-tooth-pair contact and thus a smoother transition of double- to single- to double-tooth-pair contact. This resulted in lower dynamic load factors and higher dynamic life factors. For the sets studied, the resonant speed varied with equivalent mass, mean equivalent stiffness, pressure angle, and number of teeth.

A general design chart for the dynamic life factor of a gear mesh was developed from the parametric studies (fig. 17). The objective was to determine the dynamic life factor as a single simple function of speed and contact ratio to be used when a computer and program TELSGE are not available. The heavy solid line represents the best fit of the results of the parametric studies. For $\omega/\omega_n \leq 0.5$ the dynamic life factor can be read directly from the plot by using the scale on the left. For $\omega/\omega_n > 0.5$ the dynamic life factor is the product of the value of the curve (using the scale on the right) and the contact ratio to the sixth power. The light dotted lines represent the actual results of the parametric studies and indicate the possible error when using the chart. An example problem given in appendix B demonstrates the use of the design chart. A simplified hand calculation of gear tooth stiffness is also given in appendix B.

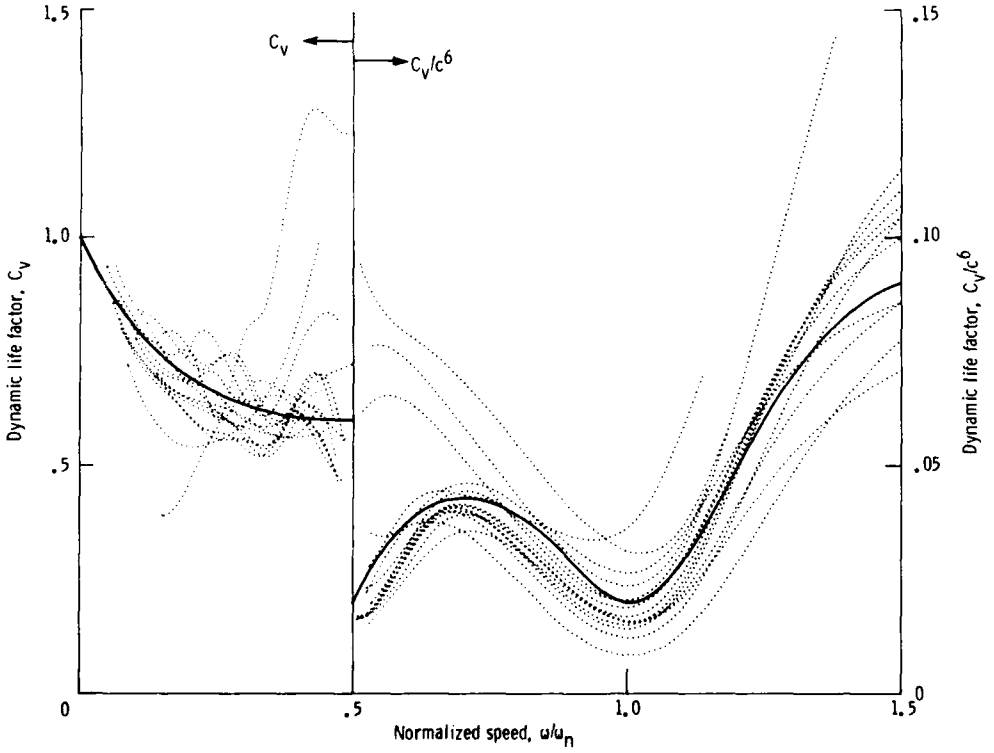

Figure 17.—Dynamic life factor.

Summary of Results

How dynamic load affects the pitting fatigue life of external spur gears was predicted by using a modified version of the NASA computer program TELSGE to perform parametric studies. TELSGE was modified to include a surface pitting fatigue life analysis. The parametric studies modeled low-contact-ratio involute gears with no tooth spacing or profile errors. The following results were obtained:

1. Gear life predictions based on dynamic loads generally differed significantly from those based on static loads and were strongly influenced by the maximum dynamic load during contact.

2. Gear mesh operating speeds strongly affected predicted dynamic loads and thus gear life. In most cases studied, meshes operating at a resonant speed or one-half the resonant speed had significantly shorter lives than the life based on static loads. Meshes operating above resonance had significant longer lives.

3. In general, meshes with higher contact ratios had higher predicted dynamic life factors than meshes with lower contact ratios.

4. Damping significantly affected predicted gear mesh life for meshes operating at or near a resonant speed or one-half the resonant speed.

5. A solution for dynamic load converged with only a few iterations of gear tooth stiffness and dynamic load because the Hertzian deflection was relatively small in comparison with the total gear tooth deflection.

Lewis Research Center
National Aeronautics and Space Administration
Cleveland, Ohio, April 3, 1986

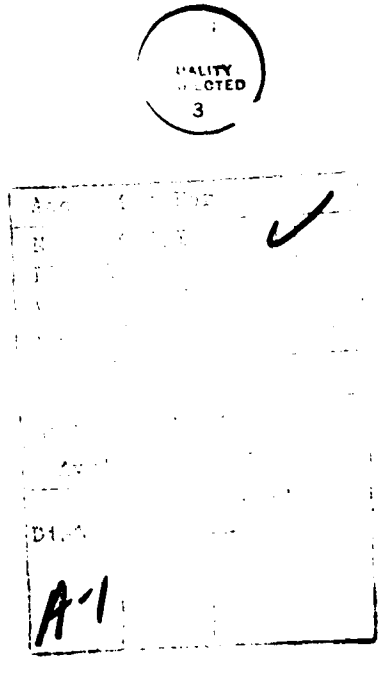

Appendix A
Symbols

B material constant (2.23×10^8 N/m$^{1.979}$, 35 000 lb/in.$^{1.979}$, ref. 21)

C_{eq} equivalent damping per unit face width, N sec/m^2 (lb sec/in.^{2})

C_v dynamic life factor

c contact ratio

d distance of inscribed parabola, m (in.)

E modulus of elasticity, Pa (psi)

e Weibull exponent

f gear tooth face width, m (in.)

h_0 tooth thickness at root radius, m (in.)

I_0 beam cross-sectional moment of inertia, m^4 (in.^{4})

i contact position index

J number of intervals; or polar mass moment of inertia per unit face width ($1/2\ mr_b^2$ for disk), kg m (lb sec^2)

j interval index

K combined stiffness per unit face width, Pa (psi)

K_{eq} equivalent stiffness per unit face width, Pa (psi)

$\bar{K}_{eq}$ mean equivalent stiffness per unit face width, Pa (psi)

k gear tooth stiffness per unit face width, Pa (psi)

L life for 90-percent probability of survival, Mrev

ℓ involute length, m (in.)

M effective mass per unit face width, J/r_b^2, kg/m (lb sec^2/in.^{2})

M_{eq} equivalent mass per unit face width, kg/m (lb sec^2/in.^{2})

m mass per unit face width, kg/m (lb sec^2/in.^{2})

m_o module, mm/tooth

N number of teeth

P diametral pitch, teeth/in.

P_d dynamic load per unit face width, N/m (lb/in.)

P_s static load per unit face width, N/m (lb/in.)

p_b base pitch, $2\pi r_b/N$, m (in.)

Q normal load, N (lb)

$\bar{Q}$ average interval load, N (lb)

Q_t tangential load, $Q \cos \varphi$, N (lb)

R radius of curvature, m (in.)

r_b base radius, $r_p \cos \varphi$, m (in.)

r_o outside radius, m (in.)

r_p pitch radius, $Nm_o/2 = N/2P$, m (in.)

r_r root radius, m (in.)

s displacement, m (in.)

T torque, N m (lb in.)

t tooth thickness at pitch radius, m (in.)

X relative displacement, m (in.)

x contact position, m (in.)

Δx interval length, m (in.)

Y Lewis form factor

Z contact length, m (in.)

z_1 contact length from pitch point to start of contact, m (in.)

z_2 contact length from pitch point to end of contact, m (in.)

α pressure angle at root radius, deg

γ density, kg/m^3 (lb/in.^{3})

δ beam deflection, m (in.)

ζ damping ratio

η life for 90-percent probability of survival, millions of stress cycles

θ angular displacement, rad

$\Sigma\rho$ curvature sum, m^{-1} (in.$^{-1}$)

$\bar{\Sigma}\rho$ average curvature sum, m^{-1} (in.$^{-1}$)

φ pressure angle, deg

ω speed, rpm

ω_n resonant speed, rpm

Subscripts:

d dynamic life

I gear tooth stiffness–dynamic load iteration index

i contact position index

j interval index

m mesh

max maximum during contact position

s static life

t tooth

1 driver gear

2 driven gear

Superscripts:

(I) first pair of teeth in contact

(II) second pair of teeth in contact

Appendix B
Example Problem

Example problem.—Determine the dynamic life factor of the mesh from the data given in table III when the driver gear is rotating at 5000 rpm.

Solution.—The pitch radii are

$$r_{p,1} = \frac{1}{2}N_1 m_o = \frac{1}{2}(32 \text{ teeth})\left(4.233 \text{ mm/tooth} \times \frac{1 \text{ cm}}{10 \text{ mm}}\right)$$
$$= 6.773 \text{ cm } (2.667 \text{ in.})$$

$$r_{p,2} = \frac{1}{2}(100 \text{ teeth})\left(4.233 \text{ mm/tooth} \times \frac{1 \text{ cm}}{10 \text{ mm}}\right)$$
$$= 21.165 \text{ cm } (8.333 \text{ in.})$$

The base radii are

$$r_{b,1} = r_{p,1} \cos \varphi = (6.773 \text{ cm}) \cos 25° = 6.138 \text{ cm } (2.417 \text{ in.})$$

$$r_{b,2} = (21.165 \text{ cm}) \cos 25° = 19.182 \text{ cm } (7.552 \text{ in.})$$

From equations (5) and (6) the contact lengths from the pitch point to the start and end of contact are

$$z_1 = \sqrt{(21.590 \text{ cm})^2 - (19.182 \text{ cm})^2}$$
$$- (21.165 \text{ cm}) \sin 25° = 0.964 \text{ cm } (0.379 \text{ in.})$$

$$z_2 = \sqrt{(7.196 \text{ cm})^2 - (6.138 \text{ cm})^2}$$
$$- (6.773 \text{ cm}) \sin 25° = 0.894 \text{ cm } (0.351 \text{ in.})$$

From equation (7) the contact length is

$$Z = (0.964 \text{ cm}) + (0.894 \text{ cm}) = 1.858 \text{ cm } (0.730 \text{ in.})$$

The base pitch is

TABLE III.—GEAR MESH DATA USED IN DYNAMIC LIFE FACTOR EXAMPLE PROBLEM

Parameter	Driver gear	Driven gear
Number of teeth	32	100
Outside radius, cm (in.)	7.196 (2.833)	21.590 (8.500)
Root radius, cm (in.)	6.246 (2.459)	20.638 (8.125)
Lewis form factor	0.433	0.521
Module, mm/tooth (Pitch, teeth/in.)	4.233 (6)	
Face width, cm (in.)	6.350 (2.500)	
Pressure angle, deg (rad)	25 (0.436)	
Tooth thickness at pitch radius, cm (in.)	0.665 (0.262)	
Modulus of elasticity, Pa (psi)	2.068×10^{11} (30×10^6)	
Density, kg/m^3 (lb/in.^{3})	7833 (0.283)	

$$p_b = \frac{2\pi r_{b,1}}{N_1} = \frac{2\pi(6.138 \text{ cm})}{32 \text{ teeth}} = 1.205 \text{ cm } (0.475 \text{ in.})$$

From equation (33) the contact ratio is

$$c = \frac{1.858 \text{ cm}}{1.205 \text{ cm}} = 1.54$$

The masses per unit face width of the driver and driven gears can be approximated by

$$m_1 = \gamma\pi r_{p,1}^2 = (7833 \text{ kg/m}^3)\pi\left(6.773 \text{ cm} \times \frac{1 \text{ m}}{100 \text{ cm}}\right)^2$$
$$= 112.886 \text{ kg/m } (1.637 \times 10^{-2} \text{ lb sec}^2/\text{in.}^2)$$

$$m_2 = (7833 \text{ kg/m}^3)\pi\left(21.165 \text{ cm} \times \frac{1 \text{ m}}{100 \text{ cm}}\right)^2$$
$$= 1102.337 \text{ kg/m } (1.598 \times 10^{-1} \text{ lb sec}^2/\text{in.}^2)$$

The effective masses per unit face width are

$$M_1 = \frac{J_1}{r_{b,1}^2} = \frac{\frac{1}{2}m_1 r_{b,1}^2}{r_{b,1}^2} = \frac{1}{2}m_1 = \frac{1}{2}(112.886 \text{ kg/m})$$
$$= 56.443 \text{ kg/m } (8.185 \times 10^{-3} \text{ lb sec}^2/\text{in.}^2)$$

$$M_2 = \frac{1}{2}(1102.337 \text{ kg/m}) = 551.169 \text{ kg/m}$$
$$(7.990 \times 10^{-2} \text{ lb sec}^2/\text{in.}^2)$$

From equation (22) the equivalent mass per unit face width is

$$M_{eq} = \frac{(56.443 \text{ kg/m})(551.169 \text{ kg/m})}{(56.443 \text{ kg/m}) + (551.169 \text{ kg/m})}$$
$$= 51.200 \text{ kg/m } (7.424 \times 10^{-3} \text{ lb sec}^2/\text{in.}^2)$$

Determining teeth stiffnesses by the methods of Cornell (ref. 17) requires the use of a computer. For this example the stiffness calculations will be simplified by modeling the gear teeth as cantilever beams of uniform strength (beams in which the section modulus varies along the beam in the same proportion as the bending moment). The pressure angles at the root radii of the driver and driven gears (fig. 18) are

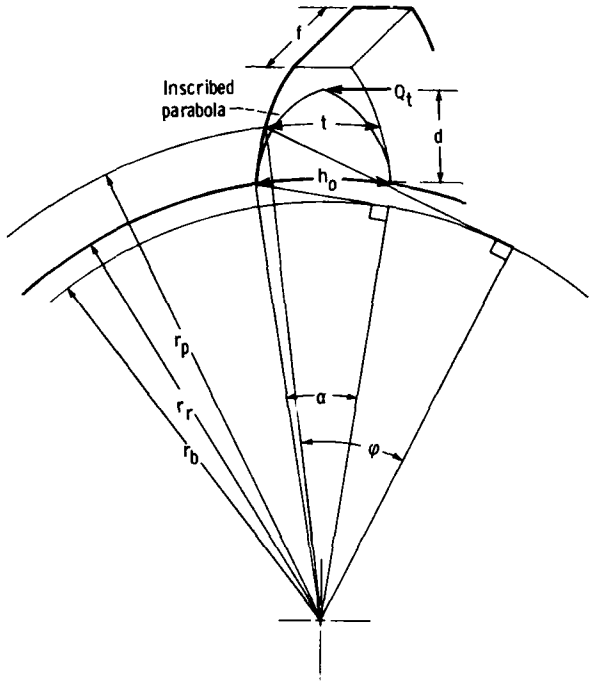

Figure 18.—Gear tooth model for simplified stiffness calculations.

$$\alpha_1 = \cos^{-1}\left(\frac{r_{b,1}}{r_{r,1}}\right) = \cos^{-1}\left(\frac{6.138\text{ cm}}{6.246\text{ cm}}\right)$$

$$= 10.670° = 0.186\text{ rad}$$

$$\alpha_2 = \cos^{-1}\left(\frac{19.182\text{ cm}}{20.638\text{ cm}}\right) = 21.651° = 0.378\text{ rad}$$

From reference 22 the tooth thickness at the pitch radius is related to the tooth thickness at the root radius by

$$t = 2r_p\left[\frac{h_0}{2r_r} + (\tan\alpha - \alpha) - (\tan\varphi - \varphi)\right]$$

Therefore the teeth thicknesses at the root radii are

$$h_{0,1} = 2r_{r,1}\left[\frac{t}{2r_{p,1}} - (\tan\alpha_1 - \alpha_1) + (\tan\varphi - \varphi)\right]$$

$$= 2(6.246\text{ cm})\left[\frac{0.665\text{ cm}}{2(6.773\text{ cm})} - (\tan 0.186 - 0.186) + (\tan 0.436 - 0.436)\right]$$

$$= 0.960\text{ cm (0.378 in.)}$$

$$h_{0,2} = 2(20.638\text{ cm})\left[\frac{0.665\text{ cm}}{2(21.165\text{ cm})} - (\tan 0.378 - 0.378) + (\tan 0.436 - 0.436)\right]$$

$$= 1.095\text{ cm (0.431 in.)}$$

From reference 23 and figure 18 the distance of the inscribed parabola is

$$d = \frac{h_0^2}{6m_oY}$$

where Y is the Lewis form factor. Thus the distances of the inscribed parabolas are

$$d_1 = \frac{h_{0.1}^2}{6m_oY_1} = \frac{(0.960\text{ cm})^2}{6\left(4.233\text{ mm/tooth} \times \frac{1\text{ cm}}{10\text{ mm}}\right)(0.433)}$$

$$= 0.838\text{ cm (0.330 in.)}$$

$$d_2 = \frac{(1.095\text{ cm})^2}{6\left(4.233\text{ mm/tooth} \times \frac{1\text{ cm}}{10\text{ mm}}\right)(0.521)}$$

$$= 0.906\text{ cm (0.357 in.)}$$

The inscribed parabola in figure 18 is a cantilever beam of uniform strength. From reference 24 the deflection for the beam is

$$\delta = \frac{2Q_t d^3}{3EI_0} \qquad \text{where } I_0 = \frac{1}{12}fh_0^3$$

The gear tooth stiffness per unit face width is

$$k = \frac{Q_t}{\delta f} = \frac{3EI_0}{2d^3f} = \frac{Eh_0^3}{8d^3}$$

For the driver and driven gears, respectively,

$$k_1 = \frac{Eh_{0,1}^3}{8d_1^3} \frac{(2.068 \times 10^{11}\text{ Pa})\left(0.960\text{ cm} \times \frac{1\text{ m}}{100\text{ cm}}\right)^3}{8\left(0.838\text{ cm} \times \frac{1\text{ m}}{100\text{ cm}}\right)^3}$$

$$= 3.886 \times 10^{10}\text{ Pa } (5.636 \times 10^6\text{ psi})$$

$$k_2 = \frac{(2.068 \times 10^{11}\ \text{Pa})\left(1.095\ \text{cm} \times \frac{1\ \text{m}}{100\ \text{cm}}\right)^3}{8\left(0.916\ \text{cm} \times \frac{1\ \text{m}}{100\ \text{cm}}\right)^3}$$

$$= 4.564 \times 10^{10}\ \text{Pa}\ (6.599 \times 10^6\ \text{psi})$$

From equation (25) the combined stiffness per unit face width is

$$K = \frac{(3.886 \times 10^{10}\ \text{Pa})(4.564 \times 10^{10}\ \text{Pa})}{(3.886 \times 10^{10}\ \text{Pa}) + (4.564 \times 10^{10}\ \text{Pa})}$$

$$= 2.099 \times 10^{10}\ \text{Pa}\ (3.040 \times 10^6\ \text{psi})$$

For this example it is assumed that the combined stiffness is constant with respect to contact position. During single-tooth-pair contact the equivalent stiffness is K. During double-tooth-pair contact the equivalent stiffness is $2K$. The mean equivalent stiffness per unit face width (fig. 19) is given as

$$\bar{K}_{eq} = \frac{1}{Z}\int_0^Z K_{eq}\,dx$$

$$= \frac{1}{Z}\left(\int_0^{Z-p_b} K_{eq}\,dx + \int_{Z-p_b}^{p_b} K_{eq}\,dx + \int_{p_b}^{Z} K_{eq}\,dx\right)$$

$$= \frac{1}{Z}\left\{2K\left[(Z-p_b) - 0\right] + K\left[p_b - (Z-p_b)\right] + 2K\left[Z - p_b\right]\right\}$$

$$= K\left[3 - 2\left(\frac{p_b}{Z}\right)\right] = K\left(3 - \frac{2}{c}\right)$$

$$= (2.099 \times 10^{10}\ \text{Pa})\left(3 - \frac{2}{1.54}\right)$$

$$= 3.571 \times 10^{10}\ \text{Pa}\ (5.172 \times 10^6\ \text{psi})$$

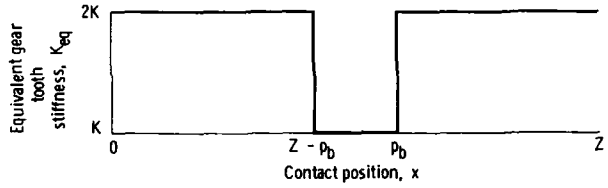

Figure 19.—Equivalent gear tooth stiffness as a function of contact position.

From equation (31) the resonant speed in terms of driver gear rotations is

$$\omega_n = \frac{\sqrt{\frac{\bar{K}_{eq}}{M_{eq}}}\cos\varphi}{N_1}\left(\frac{60}{2\pi}\right)$$

$$= \frac{\sqrt{\frac{3.571 \times 10^{10}\ \text{Pa}}{51.200\ \text{kg/m}}}\cos 25^\circ}{32\ \text{teeth}}\left(\frac{60}{2\pi}\right) = 7143\ \text{rpm}$$

At a driver operating speed of 5000 rpm

$$\frac{\omega}{\omega_n} = \frac{5000\ \text{rpm}}{7143\ \text{rpm}} = 0.70$$

From figure 17 for $\omega/\omega_n = 0.70$

$$\frac{C_v}{c^6} = 0.04$$

and the dynamic life factor is

$$C_v = 0.04\ c^6 = 0.04\ (1.54)^6 = 0.53$$

Thus about a 50-percent decrease in life compared with that using static loads is predicted for this example. Note that the simplified stiffness model used in the example may produce erroneous values for the resonant speed. The mean value of the equivalent stiffness per unit face width for this example was computed, by using Cornell's method (ref. 17) and TELSGE, as 2.741×10^{10} Pa (3.975×10^6 psi). This produced a resonant speed of 6260 rpm and a dynamic life factor of 0.56.

References

1. Surface Durability (Pitting) of Spur Gear Teeth. The American Gear Manufacturers Association (AGMA) Standard 210.02, Jan. 1965.
2. Coy, J.J.; Townsend, D.P.; and Zaretsky, E.V.: Analysis of Dynamic Capacity of Low-Contact-Ratio Spur Gears Using Lundberg-Palmgren Theory. NASA TN D-8029, 1975.
3. Townsend, D.P.; Coy, J.J.; and Zaretsky, E.V.: Experimental and Analytical Load-Life Relation for AISI 9310 Steel Spur Gears. J. Mech. Des., vol. 100, no. 1, Jan. 1978, pp. 54-60.
4. Coy, J.J.; and Zaretsky, E.V.: Life Analysis of Helical Gear Sets Using Lundberg-Palmgren Theory. NASA TN D-8045, 1975.
5. Coy, J.J.; Townsend, D.P.; and Zaretsky, E.V.: Dynamic Capacity and Surface Fatigue Life for Spur and Helical Gears. J. Lubr. Technol., vol. 98, no. 2, Apr. 1976, pp. 267-276.
6. Coy, J.J.; Townsend, D.P.; and Zaretsky, E.V.: An Update on the Life Analysis of Spur Gears. Advanced Power Transmission Technology, NASA CP-2210, G.K. Fischer, ed., 1983, pp. 421-434.
7. Buckingham, E.: Analytical Mechanics of Gears. McGraw-Hill, 1949.
8. Tuplin, W.A.: Dynamic Loads on Gear Teeth. Proceedings, International Conference on Gearing, Institution of Mechanical Engineers, London, 1958, pp. 24-30.
9. Richardson, Herbert Heath: Static and Dynamic Load, Stresses and Deflection Cycles in Spur Gear Systems. Ph.D. Thesis, Massachusetts Institute of Technology, 1958.
10. Attia, A.Y.: Dynamic Loading on Spur Gear Teeth. J. Eng. Ind., vol. 81, no. 1, Feb. 1959, pp. 1-9.
11. Ichimaru, K.; and Hirano, F.: Dynamic Behavior of Heavy-Loaded Spur Gears. J. Eng. Ind., vol. 96, no. 2, May 1974, pp. 373-381.
12. Cornell, R.W.; and Westervelt, W.W.: Dynamic Tooth Loads and Stressing for High Contact Ratio Spur Gears. J. Mech. Des., vol. 100, no. 1, Jan. 1978, pp. 69-76.
13. Kasuba, R.; and Evans, J.W.: An Extended Model for Determining Dynamic Loads in Spur Gears. J. Mech. Des., vol. 103, no. 2, Apr. 1981, pp. 398-409.
14. Wang, K.L.; and Cheng, H.S.: Thermal Elastohydrodynamic Lubrication of Spur Gears. NASA CR-3241, 1980.
15. Wang, K.L.; and Cheng, H.S.: A Numerical Solution to the Dynamic Load, Film Thickness, and Surface Temperatures in Spur Gears. Part I, Analysis. J. Mech. Des., vol. 103, no. 1, Jan. 1981, pp. 177-187.
16. Wang, K.L.; and Cheng, H.S.: A Numerical Solution to the Dynamic Load, Film Thickness, and Surface Temperatures in Spur Gears. Part II, Results. J. Mech. Des., vol. 103, no. 1, Jan. 1981, pp. 188-194.
17. Cornell, R.W.: Compliance and Stress Sensitivity of Spur Gear Teeth. J. Mech. Des., vol. 103, no. 2, Apr. 1981, pp. 447-459.
18. Lundberg, G.; and Palmgren, A.: Dynamic Capacity of Rolling Bearings, Acta Polytechnica, Mechanical Engineering Series, vol. 1, no. 3, 1947.
19. Lundberg, G.; and Palmgren, A.: Dynamic Capacity of Rolling Bearings. J. Appl. Mech., vol. 16, no. 2, June 1949, pp. 165-172.
20. Lundberg, G.; and Palmgren, A.: Dynamic Capacity of Roller Bearings. Acta Polytechnica, Mechanical Engineering Series, vol. 2, no. 4, 1952.
21. Lewicki, D.G., et al.: Fatigue Life Analysis of a Turboprop Reduction Gearbox. ASME Paper 85-DET-10, Sept. 1985. (Also NASA TM-87014.)
22. Khiralla, T.W.: On the Geometry of External Involute Spur Gears. GEARS, North Hollywood, 1976.
23. Deutschman, A.D.; Michels, W.J.; and Wilson, C. E.: Machine Design—Theory and Practice. Macmillan, 1975.
24. Timoshenko, S.: Strength of Materials. 3rd ed., Van Nostrand, 1955.

1. Report No.	2. Government Accession No.	3. Recipient's Catalog No.
NASA TP-2610 AVSCOM TR 86-C-21	AD-A170 906	

4. Title and Subtitle	5. Report Date
Predicted Effect of Dynamic Load on Pitting Fatigue Life for Low-Contact-Ratio Spur Gears	June 1986
	6. Performing Organization Code: 505-62-51

7. Author(s)	8. Performing Organization Report No.
David G. Lewicki	E-2989
	10. Work Unit No.

9. Performing Organization Name and Address	11. Contract or Grant No.
NASA Lewis Research Center and Propulsion Directorate, U.S. Army Aviation Research and Technology Activity - AVSCOM, Cleveland, Ohio 44135	
	13. Type of Report and Period Covered: Technical Paper

12. Sponsoring Agency Name and Address	14. Sponsoring Agency Code
National Aeronautics and Space Administration Washington, D.C. 20546 and U.S. Army Aviation Systems Command, St. Louis, Mo. 63120	

15. Supplementary Notes

16. Abstract

How dynamic load affects the surface pitting fatigue life of external spur gears was predicted by using NASA computer program TELSGE. Parametric studies were performed over a range of various gear parameters modeling low-contact-ratio involute spur gears. In general, gear life predictions based on dynamic loads differed significantly from those based on static loads, with the predictions being strongly influenced by the maximum dynamic load during contact. Gear mesh operating speed strongly affected predicted dynamic load and life. Meshes operating at a resonant speed or one-half the resonant speed had significantly shorter lives. Dynamic life factors for gear surface pitting fatigue were developed on the basis of the parametric studies. In general, meshes with higher contact ratios had higher dynamic life factors than meshes with lower contact ratios. A design chart was developed for hand calculations of dynamic life factors.

17. Key Words (Suggested by Author(s))	18. Distribution Statement
Spur gears Dynamic loads Pitting fatigue life	Unclassified - unlimited STAR Category 37

19. Security Classif. (of this report)	20. Security Classif. (of this page)	21. No. of pages	22. Price*
Unclassified	Unclassified	20	A02

*For sale by the National Technical Information Service, Springfield, Virginia 22161

NASA-Langley, 1986

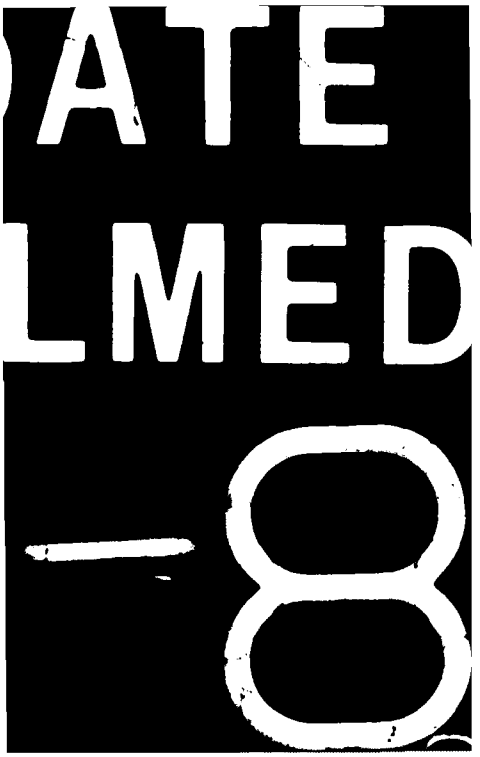
ATE
LMED
8